GEOPHYSICAL RESEARCH LETTERS, VOL. 34, L10306, doi:10.1029/2007GL029462, 2007

Click Here for Full Article

First principles investigation of the postspinel transition in Mg_2SiO_4

Yonggang G. Yu,[1] Renata M. Wentzcovitch,[1] Taku Tsuchiya,[2] Koichiro Umemoto,[1] and Donald J. Weidner[3]

Received 24 January 2007; accepted 23 April 2007; published 24 May 2007.

[1] We have investigated the dissociation of iron free ringwoodite, Mg_2SiO_4 γ-spinel, into MgO periclase and $MgSiO_3$ perovskite using quasi-harmonic free energy computations within the local density approximation (LDA) and generalized gradient approximation (GGA). The transition pressure, P_{tr}, obtained from GGA is higher and in much better agreement with experimental measurements than its LDA counterpart. This can be rationalized by close inspection of GGA and LDA functional forms. The Clapeyron slope obtained from this calculation is -2.9 – -2.6 MPa/K. Surprisingly, we find a small decrease in bulk sound velocity across this transition. Our results are consistent with 64 ± 12% ringwoodite volume fraction at the bottom of the transition zone. **Citation:** Yu, Y. G., R. M. Wentzcovitch, T. Tsuchiya, K. Umemoto, and D. J. Weidner (2007), First principles investigation of the postspinel transition in Mg_2SiO_4, *Geophys. Res. Lett.*, *34*, L10306, doi:10.1029/2007GL029462.

1. Introduction

[2] Ringwoodite, γ-spinel (Mg, Fe)$_2SiO_4$, is thought to be the most abundant mineral phase in the lower part of Earth's transition zone. Its dissociation into (Mg, Fe)O ferropericlase, and (Mg, Fe)SiO_3 perovskite, often referred to as the postspinel transition, is believed to cause the 660-km discontinuity defining the boundary between transition zone and lower mantle. Experiments [e.g., *Boehler and Chopelas*, 1991; *Akaogi and Ito*, 1993; *Irifune et al.*, 1998; *Shim et al.*, 2001; *Chudinovskikh and Boehler*, 2001; *Katsura et al.*, 2003; *Fei et al.*, 2004; *Litasov et al.*, 2005] show that this dissociation happens around 23 GPa and 1900 K. This condition gives a reference pressure and temperature for 660-km depth in mantle. According to *Ito and Takahashi* [1989], when 26 mol% or less iron is present in ringwoodite, the transition pressure changes by less than 0.15 GPa at ~1600 °C. Here we consider only the dissociation of iron free Mg_2SiO_4 ringwoodite.

[3] The exact P, T conditions of this transition, including the Clapeyron slope (CS), is still debated. Uncertainties in experimentally determined phase boundaries come from difficulties in measuring pressure (P) at high temperature (T) (e.g. pressure scale) and measuring T at high P (e.g. pressure effects on thermocouple). In addition, CS's are also very important for Geodynamic modeling. They influence the way convection, or mass flow happens across boundary layers. Negative CS's tend to inhibit convection while positive CS's tend to aid. The larger the magnitude of the negative CS's the more difficult it is for mass to flow across this boundary layer.

[4] The postspinel transition has a negative CS. The Clapeyron relation $\frac{dP}{dT} = \frac{\Delta S}{\Delta V}$ gives the slope of the phase boundary and indicates that it is negative because of an increase in entropy ($\Delta S > 0$) and a decrease in volume ($\Delta V < 0$) across the transition. This increase in entropy can be understood from changes in the vibrational density of state (VDoS) of the three relevant phases. Within the quasi-harmonic approximation (QHA), entropy is given by

$$S(V,T) = k_B \sum_{q,i} \left[\frac{\hbar\omega_{q,i}(V)/k_B T}{\left(e^{\frac{\hbar\omega_{q,i}(V)}{k_B T}} - 1\right)} - \ln\left(1 - e^{-\frac{\hbar\omega_{q,i}(V)}{k_B T}}\right) \right]. \quad (1)$$

S increases with decreasing range of ω or with a decrease in the center of mass of the VDoS [*Karki and Wentzcovitch*, 2003]. Figure 1 shows the VDoS at 20 GPa for ringwoodite (referred as rw hereafter), perovskite (referred as pv hereafter), and periclase (referred as pc hereafter). The black dots indicate the position of the VDoS's centers of mass, ω_{cm}, of the three relevant phases. ω_{cm} for rw, pv, and pc are 533.9 cm^{-1}, 517.6 cm^{-1}, and 466.3 cm^{-1} respectively. The average phonon frequency clearly decreases across this transition. This is related with an increase in average bond length across the transition.

2. Static P_{tr} by LDA and GGA

[5] Our density functional calculations use the PBE GGA [*Perdew et al.*, 1996] and the LDA [*Ceperley and Alder*, 1980] as parameterized by *Perdew and Zunger* [1981] for exchange correlation functionals in combination with the plane wave pseudopotential method. The pseudopotentials used here have been used in previous calculations of magnesium silicates [*Tsuchiya et al.*, 2004]. All static energies have converged within 10^{-4} Ry/atom. Density functional perturbation theory [*Baroni et al.*, 2001] is used to calculate phonon frequencies. These are used in conjunction with the QHA to compute the Helmholtz free energy and thermodynamic quantities of interest for each phase. The phase boundary is located by comparing Gibbs free energies of rw and pv-pc aggregate.

[6] Figure 2 shows the static energy versus volume curves for rw and for the pv-pc aggregate by LDA and GGA. The difference between LDA and GGA internal

[1]Minnesota Supercomputing Institute, Department of Chemical Engineering and Materials Science, University of Minnesota-Twin Cities, Minneapolis, Minnesota, USA.
[2]Geodynamics Research Center, Ehime University, Matsuyama, Japan.
[3]Center for High Pressure Research and Department of Geosciences, State University of New York at Stony Brook, Stony Brook, New York, USA.

Copyright 2007 by the American Geophysical Union.
0094-8276/07/2007GL029462$05.00

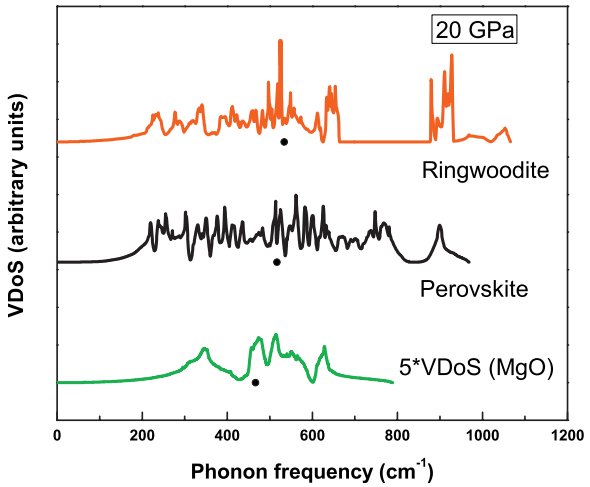

Figure 1. VDoS of rw, pv, and MgO at 20 GPa. The black dots denote the average (center of mass) frequency.

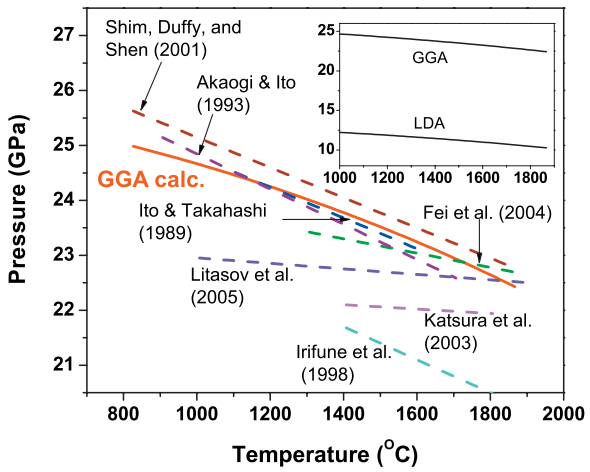

Figure 3. Computed postspinel transition boundary compared with experimental measurements. Inset compares predicted GGA and LDA phase boundaries. At 1900 K the Clapeyron slopes are in MPa/K: GGA, −2.9; LDA, −2.6; *Ito and Takahashi* [1989], −2.8; *Akaogi and Ito* [1993], −3.0; *Irifune et al.* [1998], ∼ −2.5; *Shim et al.* [2001], −2.75; *Katsura et al.* [2003], ∼ −2 − −0.4; *Fei et al.* [2004], −1.3; *Litasov et al.* [2005], −0.5.

energies is denoted by ΔE and is marked by arrows. This difference is approximately given by the following functional of density, $n(\vec{r})$

$$\Delta E[n] = E_{XC}^{GGA} - E_{XC}^{LDA} \approx E_{X}^{GGA} - E_{X}^{LDA} = -\frac{3e^2\mu}{8\pi}\int d^3r\,\frac{|\nabla n|}{\frac{\mu}{\kappa}s+\frac{1}{s}}, \quad (2)$$

where $s = |\nabla n| / (2k_F n)$ and $k_F = (3\pi^2 n)^{1/3}$, with parameters $\mu \approx 0.21951$ and $\kappa \approx 0.804$ [*Perdew et al.*, 1996]. Here we have neglected contributions from changes in correlation energy, kinetic energy, and interaction with the external potential, since these are usually at least one order of magnitude smaller than exchange energy term. (For materials at typical solid state densities, $r_s = (3/4\pi n)^{1/3} \approx 2 - 6\ a_B$ (Bohr radius), $\epsilon_x = -1.832/r_s$ Har (Hartree) for exchange energy, but for Wigner correlation energy $\epsilon_c = -0.44/(r_s + 7.8)$ Har, which is about an order of magnitude smaller.) When density decreases ($n\downarrow$), in general the density gradient increases ($|\nabla n|\uparrow$), the reduced gradient increases ($s\uparrow$). Equation 2 then indicates that when $s \in [0, \sqrt{\kappa/\mu} \approx 2]$, a common situation in the solid state, the whole integrand increases ($|\nabla n| / (\mu s/\kappa + 1/s)\uparrow$). In short, the larger the volume, the larger the energy difference $\Delta E[n]$ between LDA and GGA. Therefore, (1) for one single phase, the GGA equilibrium volume is larger than the LDA, $V_0^{GGA} > V_0^{LDA}$; (2) in case of two different phases, GGA lowers more the energy of the less dense phase (low P phase) than of the denser one (high P phase). Thus the magnitude of the common tangent is larger in the GGA

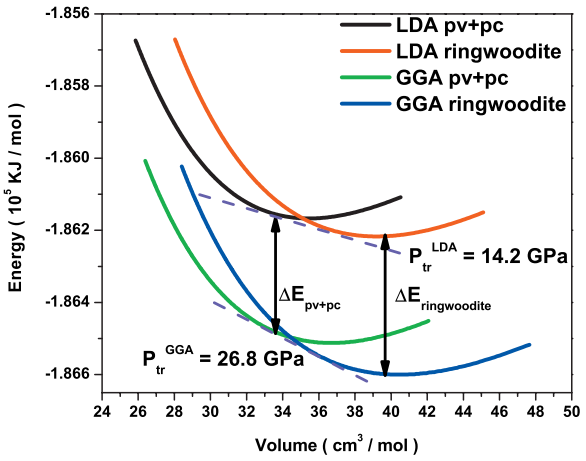

Figure 2. Static energy versus volume for rw and for pv + pc aggregate using the LDA and the GGA. The slopes of the common tangents are the transition pressures.

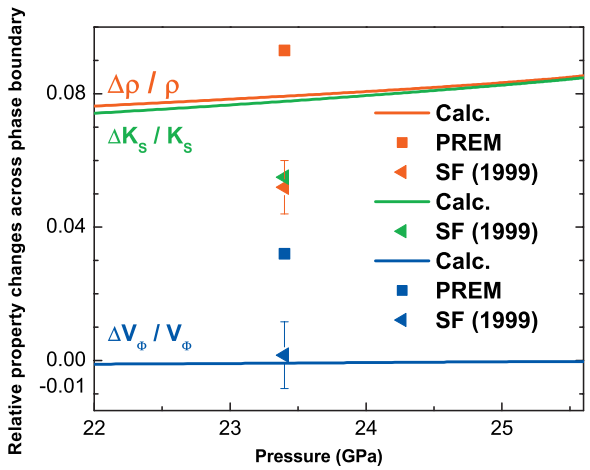

Figure 4. Percent changes in ρ, K_S, and V_Φ along the GGA phase boundary. Temperature varies with pressure as indicated in Figure 3. $\Delta x/x \equiv (x_{pv+pc} - x_{rw})/[(x_{pv+pc} + x_{rw})/2]$ for $x = \rho$, K_S, and V_Φ.

Table 1. Results Used to Calculate Jumps in ρ, K_S, and V_ϕ at T = 1900 K and P = 23.2 GPa, a Point Representative of 660-Km Condition

	Volume, Å^3	K_S, GPa
MgO-pc (calc.)	69.79(4)	232.5
Mg-pv (calc.)	156.53(4)	279.7
rw (calc.)	490.06(8)	261.1

calculation (26.8 GPa) than in LDA (14.2 GPa). This is the origin of the higher GGA transition pressure.

3. Postspinel Transition Boundary

[7] Figure 3 compares the GGA phase boundary (bold red line) with experimental measurements. The inset shows the phase boundaries determined from GGA and LDA calculations. As shown, the GGA phase boundary agrees much better with experimental measurements than the LDA boundary. The latter underestimates the transition pressure by as much as 12 GPa. Our GGA calculation predicts that at 1900 K, P_{tr}^{GGA} = 23.2 GPa and $dP/dT = -2.9$ MPa/K. In terms of CS, this GGA result is very close to the work by *Ito and Takahashi* [1989], *Akaogi and Ito* [1993], *Irifune et al.* [1998], *Shim et al.* [2001], and *Chudinovskikh and Boehler* [2001], but differs from the more recent results [e.g., *Fei et al.*, 2004; *Litasov et al.*, 2005] where smaller CS's are reported, $-1.3 - -0.4$ MPa/K. Figure 3 also indicates that in general calculated and experimental phase boundaries agree better at high T than at low T. The discrepancies even among experiments at lower T probably result from the slow kinetics of this dissociation reaction and from finite observation times. First principles calculations avoid the kinetics issue and may offer a more reliable estimate of this phase boundary. It happens that structural properties computed with the LDA are in considerably better agreement with experimental measurements than those computed with the GGA. So we use the LDA to compute property changes across the GGA phase boundary.

4. Discontinuities Across the Phase Boundary

[8] Now we investigate the contribution from rw's dissociation to the mantle discontinuity. We compute relative changes in density ρ, adiabatic bulk modulus K_S, and bulk sound velocity V_Φ, at conditions expected at 660-km and compare with seismic observations. Using bulk moduli of each single phase, we obtain the Voigt-Reuss-Hill (VRH) average bulk modulus [e.g., *Avseth et al.*, 2005] of the pv-pc aggregate. The pressure dependences of relative changes in ρ, K_S, and V_ϕ, $\Delta x/x \equiv (x_{pv+pc} - x_{rw})/[(x_{pv+pc} + x_{rw})/2]$ for $x = \rho$, K_S, and V_Φ, with $V_\Phi = (K_S/\rho)^{1/2}$ along the GGA phase boundary (Figure 3) are shown in Figure 4 together with data from PREM (squares) [*Dziewonski and Anderson*, 1981] and from the seismic impedance study (triangles) by *Shearer and Flanagan* [1999] (SF). PREM is a spherically averaged model and is likely to be less accurate than the impedance study by SF. Our result is close to the latter, especially for $\Delta V_\Phi/V_\Phi$, which falls within possible uncertainties by them (Figure 4). Properties of these phases used in the calculations of these discontinuities are shown in Tables 1 and 2.

[9] Since the mantle is expected to contain at least 35–40% in volume of other phases (e.g. majorite-garnet, Ca-pv, clinopyroxene, etc.), it is not possible to compare directly these results with the magnitude of the discontinuities in the mantle. However, it is possible to incorporate the effect of the presence of other phases into estimate of the contribution of rw's dissociation to the 660-km discontinuity as a function of its volume fraction. Here two likely scenarios emerge: (1) the dissociation reaction does not affect the stability of other phases present (pv (including Fe-, Ca-pv etc) and majorite-garnet); (2) the equilibrium of the garnet/pv system is altered by the sudden generation of alumina free pv resulting from rw's dissociation. Next we examine the discontinuities produced according to the first scenario. Investigation of the second scenario should wait until more detailed information on the garnet/pv system is available.

[10] The 660-km discontinuity should be produced primarily by rw's dissociation. However, the extent to which the dissociation disturbs thermodynamic equilibrium and induces changes in the coexisting garnet/pv system is still unclear. For a non-interacting aggregate, the relative density change at 660-km can be expressed as,

$$\frac{\Delta\rho}{\rho} \equiv \frac{\rho_{pv+pc+others} - \rho_{rw+others}}{\left(\rho_{pv+pc+others} + \rho_{rw+others}\right)/2} = \frac{2y}{\frac{2}{1-\beta} - y}. \quad (3)$$

Here $y = V_{rw}/V_{rw+others}$ is the rw volume fraction; "others" means all mineral phases other than rw or its dissociation products; $\beta = V_{pv+pc}/V_{rw}$ depends on the P, T condition at the phase boundary (e.g. β = 0.9225, 0.9236, and 0.9248 at 1600 K, 1800 K, and 2000 K respectively). Thus, $\Delta\rho/\rho$ is a function of x and T (P depends on T along the boundary).

[11] Figure 5 shows $\Delta\rho/\rho$ as a function of rw volume fraction, y, at 660-km depth. The middle black solid line is calculated at 1800 K (23.4 GPa). The upper and lower bound estimates of $\Delta\rho/\rho$ correspond to uncertainty of ±200 K on the phase boundary (see Figure 5). A density

Table 2. Calculated Properties at 1900 K and 23.2 GPa Compared With Properties Across the 660-Km Discontinuity[a]

	ρ, g/cm^3			K_S, GPa			V_ϕ, km/s		
	calculated	PREM	SF	calculated	PREM	SF	calculated	PREM	SF
Upper 660 (rw)	3.81	3.99	-	261.1	255.8	-	8.274	8.007	-
Lower 660 (pv + pc)	4.13	4.38	-	282.1 ± 2.8	299.4	-	8.266 ± 0.080	8.268	-
% Δ (rw → pv + pc)	7.9%	9.3%	5.2%	7.7 ± 1.0%	15.9%	5.5%	−0.10 ± 0.48%	3.2%	0.16%

[a]The VRH average is used to calculate the polycrystalline bulk modulus. Uncertainties are estimated from the Voigt and Reuss bounds. Values in parenthesis represent calculations from rw → pv + pc. Here % $\Delta = \Delta x/x_{av}$, $\Delta x = x_{pv+pc} - x_{rw}$ and $x_{av} = (x_{pv+pc} + x_{rw})/2$, with $x = \rho$, K_S, and V_Φ. SF, *Shearer and Flanagan* [1999].

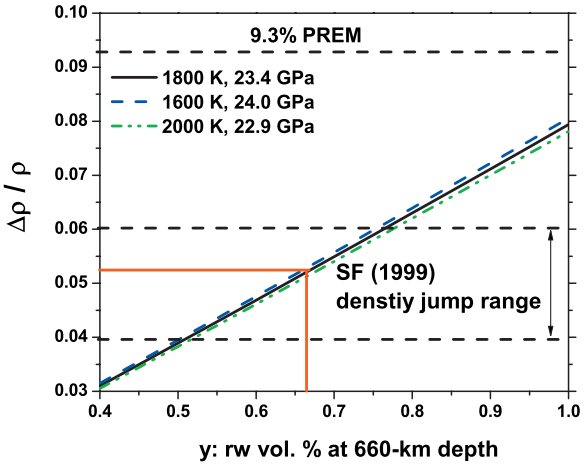

Figure 5. Density discontinuity versus rw volume fraction at 660-km for *PT*s along the phase boundary. Seismic data from PREM and from the impedance study by *Shearer and Flanagan* [1999] (SF) are also shown.

discontinuity of ~4–6%, as obtained in the impedance study by *Shearer and Flanagan* [1999], could be produced solely by the dissociation if rw volume fraction were 52 vol% < y < 76 vol%. This is in agreement with ~60% rw volume fraction in pyrolite mantle model [*Ita and Stixrude*, 1992]. However, the density discontinuity of 9.3% given by PREM cannot be produced solely by rw's dissociation, but requires simultaneous changes in the co-existing garnet/pv aggregate.

5. Discussion and Summary

[12] The GGA reproduces much better experimental phase boundaries than the LDA. Our results indicate that rw should dissociate at ~T = 1900 K at ~P = 23.2 GPa, with dP/dT = −2.9 MPa/K. We also find that V_Φ should decrease slightly across the postspinel transition. This is consistent with a seismic wave impedance study [*Shearer and Flanagan*, 1999]. Assuming that rw's dissociation plays the dominant role in creating the 660-km discontinuity we estimate that the volume fraction of rw should fall in the range 52%–76% in order to reproduce the density discontinuity of 4–6% obtained in the impedance study. The presence of iron in rw will not change this density discontinuity, assuming the effect of iron on rw and pv volumes are of second order. In case the interaction between the rw/pv-pc and the garnet/pv systems is non-negligible, the density discontinuity should increase. The presence of aluminum-free pv produced by the dissociation should draw the garnet/pv equilibrium towards pv. The presence of OH in the transition zone minerals may also influence the phase transitions at 660-km. More thorough and detailed studies of transition zone minerals are still needed for a full understanding of the nature of the 660-km discontinuity.

[13] **Acknowledgments.** YGY thanks J. Tsuchiya, B. Li, and L. Wang for useful discussions. RMW & YGY thank the hospitality and support of the Department of Geosciences and the Department of Physics and Astronomy at SUNY at Stony Brook during the writing of this paper. Research supported by NSF/EAR 013533, 0230319, and NSF/ITR 0428774 (VLab).

References

Akaogi, M., and E. Ito (1993), Refinement of enthalpy measurement of $MgSiO_3$ perovskite and negative pressure-temperature slopes for perovskite-forming reactions, *Geophys. Res. Lett.*, *20*, 1839–1842.

Avseth, P., T. Mukerji, and G. Mavko (2005), *Quantitative Seismic Interpretation: Applying Rock Physics Tools to Reduce Interpretation Risk*, Cambridge Univ. Press, New York.

Baroni, S., S. de Gironcoli, A. Dal Corso, and P. Giannozzi (2001), Phonons and related crystal properties from density-functional perturbation theory, *Rev. Mod. Phys.*, *73*, 515–562.

Boehler, R., and A. Chopelas (1991), A new approach to laser heating in high pressure mineral physics, *Geophys. Res. Lett.*, *18*, 1147–1150.

Ceperley, D. M., and B. J. Alder (1980), Ground state of the electron gas by a stochastic method, *Phys. Rev. Lett.*, *45*, 566–569.

Chudinovskikh, L., and R. Boehler (2001), High-pressure polymorphs of olivine and the 660-km seismic discontinuity, *Nature*, *411*, 574–577.

Dziewonski, A. M., and D. L. Anderson (1981), Preliminary reference Earth model, *Phys. Earth Planet. Inter.*, *25*, 297–356.

Fei, Y., J. Van Orman, J. Li, W. van Westrenen, C. Sanloup, W. Minarik, K. Hirose, T. Komabayashi, M. Walter, and K. Funakoshi (2004), Experimentally determined postspinel transformation boundary in Mg_2SiO_4 using MgO as an internal pressure standard and its geophysical implications, *J. Geophys. Res.*, *109*, B02305, doi:10.1029/2003JB002562.

Irifune, T., et al. (1998), The postspinel phase boundary in Mg_2SiO_4 determined by in situ X-ray diffraction, *Science*, *279*, 1698–1700.

Ita, J., and L. Stixrude (1992), Petrology, elasticity, and composition of the mantle transition zone, *J. Geophys. Res.*, *97*, 6849–6866.

Ito, E., and E. Takahashi (1989), Postspinel transformations in the system Mg_2SiO_4–Fe_2SiO_4 and some geophysical implications, *J. Geophys. Res.*, *94*, 10,637–10,646.

Karki, B. B., and R. M. Wentzcovitch (2003), Vibrational and quasiharmonic thermal properties of CaO under pressure, *Phys. Rev. B*, *68*, 224304, doi:10.1103/PhysRevB.68.224304.

Katsura, T., et al. (2003), Post-spinel transition in Mg_2SiO_4 determined by high P-T in situ X-ray diffractometry, *Phys. Earth Planet. Inter.*, *136*, 11–24.

Litasov, K., E. Ohtani, A. Sano, A. Suzuki, and K. Funakoshi (2005), In situ X-ray diffraction study of post-spinel transformation in a peridotite mantle: Implication for the 660-km discontinuity, *Earth Planet. Sci. Lett.*, *238*, 311–328.

Perdew, J. P., and A. Zunger (1981), Self-interaction correction to density-functional approximations for many-electron systems, *Phys. Rev. B*, *23*, 5048–5079.

Perdew, J. P., K. Burke, and M. Ernzerhof (1996), Generalized gradient approximation made simple, *Phys. Rev. Lett.*, *77*, 3865–3868.

Shearer, P. M., and M. P. Flanagan (1999), Seismic velocity and density jumps across the 410- and 660-kilometer discontinuities, *Science*, *285*, 1545–1548.

Shim, S. N., T. S. Duffy, and G. Shen (2001), The post-spinel transformation in Mg_2SiO_4 and its relation to the 660-km seismic discontinuity, *Nature*, *411*, 571–574.

Tsuchiya, T., J. Tsuchiya, K. Umemoto, and R. M. Wentzcovitch (2004), Phase transition in $MgSiO_3$ perovskite in the Earth's lower mantle, *Earth Planet. Sci. Lett.*, *224*, 241–248.

T. Tsuchiya, Geodynamics Research Center, Ehime University, Bunkyo-cho 2-5, Matsuyama 790-8577, Japan.

K. Umemoto, R. M. Wentzcovitch, and Y. G. Yu, Minnesota Supercomputing Institute, Department of Chemical Engineering and Materials Science, University of Minnesota-Twin Cities, Minneapolis, MN 55455, USA. (yonggang@cems.umn.edu)

D. J. Weidner, Center for High Pressure Research and Department of Geosciences, State University of New York at Stony Brook, Stony Brook, NY 11794, USA.